The typical shear mode of failure for the tested channels for channel specimens with openings in web is depicted in Fig. 4. It was observed from Fig. 4 that for the channels particularly with offset web openings, the top flanges were pulled down and slightly distorted. This is due to distortional buckling and unbalanced shear flow in channels with unrestrained flanges, which is consistent with previous work by Keerthan and Mahendran (2013) on cold-formed carbon steel lipped channels. As a result of this combined shear and flange distortion phenomena, the shear strength of channels with offset openings are generally less than channels with centred openings. The experimental results are presented in Table 1. To provide more information, Fig. 5 and Fig. 6 show load-vertical displacement curves from tested channels 175×60-t1.5 and 200×75-t1.5 with web openings subjected to shear loads.

Table 1 Measured channel specimen details and experimental and FE ultimate shear strengths

Channel	Web height	Flange width	Web thickness	Web opening diameter	Aspect ratio	Full pair experimental ultimate load	Single web experimental ultimate load	Single web FE load	Comparison
	d	b_f	t	a	s/d	V_{LAB}	V_{LAB}	V_{FEA}	V_{LAB}/V_{FEA}
	(mm)	*(mm)*	*(mm)*	*(mm)*		*(kN)*	*(kN)*	*(kN)*	
175x60-t1.5-A0	175.60	60.12	1.50	0.0	1.0	149.72	37.43	37.64	0.99
175x60-t1.5-A0	175.24	60.22	1.48	0.0	1.0	147.36	36.84	37.12	0.99
175x60-t1.5-A0	175.37	60.34	1.49	0.0	1.0	148.48	37.12	37.65	0.99
175x60-t1.5-MA0.2	175.55	59.93	1.49	32.79	1.0	138.04	34.51	34.95	0.99
175x60-t1.5-MA0.4	175.39	59.94	1.48	67.25	1.0	96.28	24.07	24.35	0.99
175x60-t1.5-OA0.2	175.47	59.96	1.48	32.78	1.0	125.64	31.41	31.65	0.99
175x60-t1.5-OA0.4	175.56	59.91	1.50	69.02	1.0	95.36	23.84	23.97	0.99
200x75-t1.5-A0	200.39	75.07	1.49	0.0	1.0	154.68	38.67	38.94	0.99
200x75-t1.5-A0	200.36	75.16	1.49	0.0	1.0	153.72	38.43	38.64	0.99
200x75-t1.5-A0	200.45	75.28	1.48	0.0	1.0	152.64	38.16	38.49	0.99
200x75-t1.5-MA0.2	200.21	75.02	1.50	37.47	1.0	140.6	35.15	35.95	0.98
200x75-t1.5-MA0.4	200.36	75.07	1.48	76.99	1.0	99.64	24.91	25.26	0.99
200x75-t1.5-OA0.2	200.76	74.85	1.50	41.53	1.0	129.72	32.43	32.78	0.99
200x75-t1.5-OA0.4	200.76	74.85	1.48	77.14	1.0	99.72	24.93	25.12	0.99
250x75-t1.5-A0	250.25	74.95	1.48	0.0	1.0	157.84	39.46	38.65	1.02
250x75-t1.5-A0	250.00	75.32	1.49	0.0	1.0	158.44	39.61	38.95	1.02
250x75-t1.5-A0	250.00	75.45	1.48	0.0	1.0	157	39.25	38.44	1.02
250x75-t1.5-MA0.2	250.14	75.02	1.48	49.44	1.0	129.84	32.46	31.75	1.02
250x75-t1.5-MA0.4	250.32	75.06	1.50	96.45	1.0	91.04	22.76	22.12	1.03
250x75-t1.5-OA0.2	250.11	75.04	1.49	49.43	1.0	129	32.25	31.95	1.01
250x75-t1.5-OA0.4	250.08	75.03	1.48	93.91	1.0	98.64	24.66	24.05	1.02
Mean									1.00
CoV									0.02

3. NUMERICAL INVESTIGATION

The general-application finite element (FE) programme package ABAQUS (2014) was used for the numerical investigation to model the test arrangement comprising of channel-sections and load and support blocks. The material nonlinearity and initial geometric imperfection were considered in the numerical modelling and cross sectional dimensions of the channels were based on the values measured in the lab. In this study, consistent with previous research by Mohammadjani et al. (2017) and Natário et al. (2014) for explicit applications, quasi-static analysis was adopted based on implicit integration procedure. The advantages of such analysis method for cold-formed stainless steel beams is the consideration of of complex material behaviour as presented by Yousefi et al. (2018a,bc,d; 2019b). Details of of the FE models are described below.

The channel-sections were modelled using the S4R thin shell element available in ABAQUS (2018) library as it is suitable for most applications particularly for complex buckling analysis of thin-walled elements. The load and support blocks were modelled applying general application C3D8R element, which has strain and plasticity capabilities and can also take into account large deflection effects. The engineering material curve from coupon tests were converted to true material curve as per equations in ABAQUS manual (2018) and applied to the models. Fig. 3 (b)) shows the FE models for the channels with openings in web under shear. To reduce the computational time, only half of the test set-ups were modelled as the pair C sections were in symmetry about their principal axes. The typical finite element meshes for the channel-sections and load and support blocks are illustrated in Fig. 3 (b). The mesh size for channel models was of 5×5 mm, while for load and support blocks the mesh size of 8×8 mm was used. Finer mesh size was used in the conjunction of flanges and web.

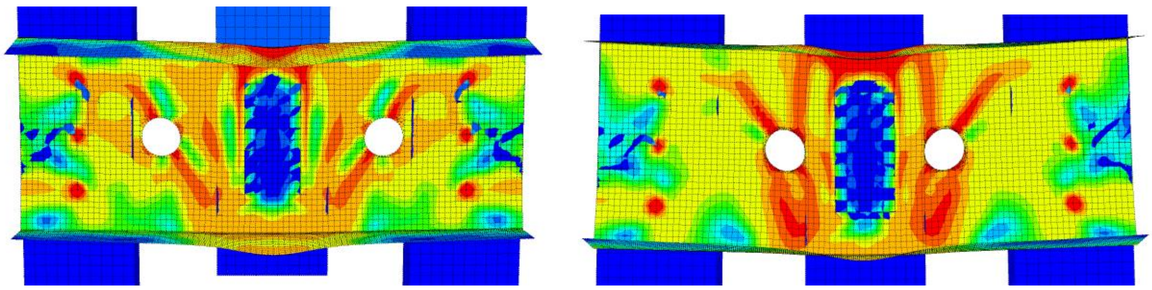

(a) Centred web openings (b) Offset web openings

Fig. 7 FEA shear modes of failure for channels with a/h=0.2 web opening ratio

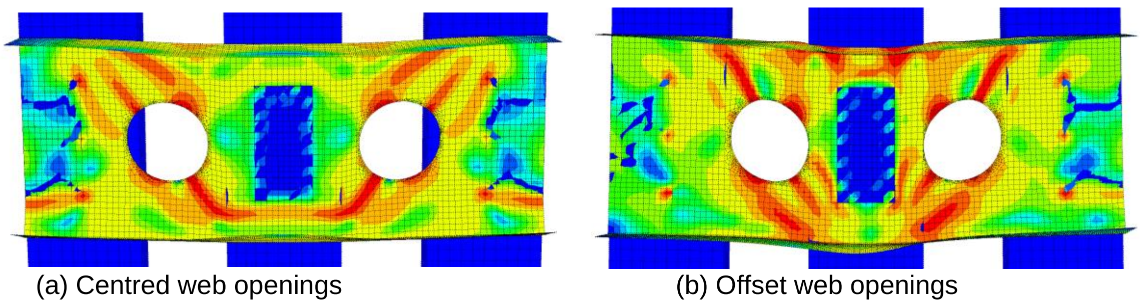

(a) Centred web openings (b) Offset web openings

Fig. 8 FEA shear modes of failure for channels with a/h=0.4 web opening ratio

The channel specimens were loaded through the load transverse block by using displacement control. A referencing point constraining top surfaces was added on top of the load block to apply the vertical displacement. The nodes on symmetry surfaces were prevented from translating in the x direction and rotating about the y and z axes. In order to simulate the connection of washer plate to the pair channel and the support and load blocks, a combination of Cartesian connector, "CONN3D2" and "tie constraint" was used. The interface contacts between the supports and load block and channels were simulated using *surface to surface* option contact in ABAQUS (2018). In this case, the web of the channels were considered as *slave surface* while load or support blocks as *master surface*. In all the contact surfaces, no penetration was allowed and hard frictionless contact response was considered.

Initial geometric imperfection could affect ultimate capacity and stability response of cold-formed steel channels under shear load (Pham and Hancock (2010)). In order to accurately capture and model the physical response of tested channels in the experimental investigation, initial geometric imperfection was considered in the FE models. Different methods of incorporating initial imperfection are available in ABAQUS manual (2018). One of these methods is to use the buckling analysis to create the possible modes and nodal displacement of these nodes. The lowest mode shape under the shear loading was then assumed as the initial imperfection pattern Gardner and Nethercot (2004). The considered local imperfection value was based on the predictive equation (1) investigated by the Gardner and Nethercot (2004) for the use in cold-formed stainless steels. Where in the following equation (1), σ_(cr,min) considered as the elastic critical buckling stress of the related most slender plate of the channels.

$$\omega_0 = 0.023\left(\frac{\sigma_{0.2}}{\sigma_{cr,min}}\right) \quad (1)$$

The FE model results and experimental results have been compared to verify the accuracy of the developed FE models. The comparison of ultimate shear loads for single web from experimental and numerical results (V_{LAB} and V_{FEA}) are presented in Table 1. It can be seen that the results are in very good agreement for all the models. The mean ratio of the V_{LAB}/V_{FEA} is equal to 1.00, having the variation coefficient of equal to 0.02. The maximum differences were observed for 200×75-t1.5-MA0.2 and 250×75-t1.5-MA0.4 between experimental and numerical results; and in both cases the error was less than 3%. Furthermore, the shear failure modes of the tested channel specimens are compared against the FE predictions, as depicted in Fig. 7 and Fig. 8. The results confirm that the developed FE models could predict the failure mode of the specimens accurately. Finally, experimental and FEA load-displacement curves are compared for channels C175 and C200 in Fig. 5 and Fig. 6. A very good agreement is observed between the experimental measurements and FE results for both loading cases.

3. CONCLUSIONS

In this paper, a combination of tests and non-linear finite element analyses was used to investigate the effect of such web openings on the shear strength of cold-formed ferritic stainless steel channels; the cases of the web openings were placed either centred at mid-span or offset to the applied load are considered. The results of 21 shear tests on pair channels loaded at mid-length with span aspect ratio of 1.0 were presented. In terms of channels with web openings, the openings were placed either centred at mid-span or offset to the applied load. Quasi-static Finite Element (FE) model, considering material nonlinearity and initial geometric imperfection, was then developed and validated against experimental test results. Good agreement between the tests and finite element analyses was obtained in terms of failure load, failure modes and post-buckling behaviour.

REFERENCES

ABAQUS (2018) *Analysis User's Manual-Version 6.20*. ABAQUS Inc., USA.

Cashell, K.A. and Baddoo, N.R. (2014), "Ferritic stainless steels in structural applications", *Thin-Wall. Struct.,* **83**,169-181

Gardner, L. (2019), "Stability and design of stainless steel structures–Review and outlook", *Thin-Wall. Struct.,* **141**, 208-216.

Gardner, L. and Nethercot, D.A. (2004), "Numerical modeling of stainless steel structural components—a consistent approach", *J. Struct. Eng.,* **130** (10), 1586-1601.

Korvink, S.A., Van Den Berg, G.J. and Van Der Merwe, P. (1995), "Web Crippling Of Stainless Steel Cold-Formed Beams", *J. Constr. Steel Res.,* **34**, 225-248.

Lawson, R.M., Basta, A. and Uzzaman A. (2015), "Design of stainless steel sections with circular openings in shear, *J. Constr. Steel Res.,* **112**, 228-241.

Mohammadjani, C., Yousefi, A.M., Cai, S.Q., Clifton, G.C. and Lim, J.B.P. (2017), "Strength and stiffness of cold-formed steel portal frame joints using quasi-static finite element analysis", *Steel Compos. Struct., Int. J.*, **25**, 727-734.

Natário, P.N., Silvestre, N. and Camotim, D. (2014), "Web crippling failure using quasi-static FE models", *Thin-Wall. Struct.,* **84**, 34-49.

Poologanathan, K. and Mahendran, M. (2013), "Experimental studies of the shear behaviour and strength of lipped channel beams with web openings", *Thin-Wall. Struct.,* **73**, 131-144.

Pham, C.H. and Hancock, G.J. (2010), "Numerical simulation of high strength cold-formed purlins in combined bending and shear", *J. Constr. Steel Res.,* **66**, 1205-1217.

Pham, S.H., Pham, C.H. and Hancock G.J. (2017), "Direct strength method of design for channel sections in shear with square and circular web holes", *J. Struct. Eng.,* **143** (6) 04017017.

Pham, S.H., Pham, C.H., Rogers, C.A. and Hancock, G.J. (2019), "Shear Strength Experiments and Design of Cold-Formed Steel Channels with Web Holes", *J. Struct. Eng.,* **146** (1) 04019173.

Poologanathan, K. and Mahendran, M. (2014), "Improved shear design rules for lipped channel beams with web openings", *J. Constr. Steel Res.,* **97**, 127-142.

Rezvani, F.H., Yousefi, A.M. and Ronagh, H.R. (2015), "Effect of span length on progressive collapse behaviour of steel moment resisting frames", *Structures,* 3, 81-89.

Wanniarachchi, K.S., Mahendran, M. and Poologanathan, K. (2017), "Shear behaviour and design of Lipped Channel Beams with non-circular web openings", *Thin-Wall. Struct.,* **119**, 83-102.

Yousefi, A.M., Lim, J.B.P., Uzzaman, A., Lian, Y., Clifton, G.C. and Young, B. (2016), "Web Crippling Strength of Cold-Formed Stainless Steel Lipped Channel-Sections with Web Holes Subjected to Interior-One-Flange Loading Condition", *Steel Compos. Struct., Int. J.*, **21**, 629-659.

Yousefi, A.M., Lim, J.B.P., Uzzaman, A., Lian, Y., Clifton, G.C. and Young, B. (2017a), "Design of Cold-Formed Stainless Steel Lipped Channel-Sections with Web Holes Subjected to Web Crippling Under End-One-Flange Loading Condition", *Advances in Structural Eng.,* **20**, 1024-1045.

Yousefi, A.M., Uzzaman, A., Lim, J.B.P., Clifton, G.C. and Young, B. (2017b), "Numerical Investigation of Web Crippling Strength in Cold-Formed Stainless Steel Lipped Channels with Web Holes Subjected to Interior-Two-Flange Loading Condition", *Steel Compos. Struct., Int. J.*, **23**, 363-383.

Yousefi, A.M., Uzzaman, A., Lim, J.B.P., Clifton, G.C. and Young, B (2017c), "Web Crippling Strength of Cold-Formed Stainless Steel Lipped Channels with Web Perforations Under End-Two-Flange Loading", *Advances in Struct. Eng.,* **20**, 1845-1863.

Yousefi, A.M., Lim, J.B.P. and Clifton, G.C. (2017d), "Web Bearing Capacity of Unlipped Cold-Formed Ferritic Stainless Steel Channels with Perforated Web Subject to End-Two-Flange (ETF) Loading", *Eng. Struct.* **152**, 804-818.

Yousefi, A.M., Lim, J.B.P. and Clifton, G.C. (2017e), "Cold-Formed Ferritic Stainless Steel Unlipped Channels with Web Holes Subjected to Web Crippling Under Interior-Two-Flange Loading Condition - Part I: Tests and Finite Element Model Validation", *Thin-Wall. Struct.,* **116**, 333-341.

Yousefi, A.M., Lim, J.B.P. and Clifton, G.C. (2017f), "Cold-Formed Ferritic Stainless Steel Unlipped Channels with Web Holes Subjected to Web Crippling Under Interior-Two-Flange Loading Condition - Part II: Parametric Study and Design Equations", *Thin-Wall. Struct.,* **116**, 342-356.

Yousefi, A.M., Lim, J.B.P. and Clifton, G.C. (2018a), "Web Crippling Behaviour of Unlipped Cold-Formed Ferritic Stainless Steel Channels Subject to One-Flange Loading", *J. Struct. Eng.,* ASCE **144**(8), 04018105.

Yousefi, A.M., Lim, J.B.P. and Clifton, G.C. (2018b), "Cold-Formed Ferritic Stainless Steel Unlipped Channels with Web Perforations Subject to Web Crippling Under One-Flange Loadings", *Construct. and Build. Mat.,* **191**, 713-725.

Yousefi, A.M., Lim, J.B.P. and Clifton, G.C. (2018c), "Web Bearing Capacity of Cold-Formed Ferritic Stainless Steel Unlipped Channels with Web perforations under the End-Two-Flange (ETF) Loading", *CCFSS Proceed. of Int. Specialty Conf. on Cold-Formed Steel Struct.,* Missouri University of Science and Technology, USA. https://scholarsmine.mst.edu/isccss/24iccfss/session2/1

Yousefi, A.M., Lim, J.B. and Clifton, G.C. (2018d), "Web Crippling Behavior of Cold-Formed Ferritic Stainless Steel Unlipped Channels under Interior-One-Flange And End-One-Flange Loadings", *CCFSS Proceed. of Int. Specialty Conf. on Cold-Formed Steel Struct.,* Missouri University of Science and Technology, USA. https://scholarsmine.mst.edu/isccss/24iccfss/session2/2

Yousefi, A.M., Lim, J.B.P. and Clifton, G.C. (2019a), "Web Crippling Design of Cold-Formed Ferritic Stainless Steel Unlipped Channels with Fastened Flanges Under End-Two-Flange Loading", *J. of Construct. Steel Research,* **152**, 12-28.

Yousefi, A.M., Lim, J.B.P. and Clifton, G.C. (2019b), "Web Crippling Strength of Perforated Cold-Formed Ferritic Stainless Steel Unlipped Channels with Restrained Flanges Under One-Flange Loadings", *Thin-Wall. Struct.,* 137, 94-105.

Yousefi, A.M. and Samali, B. (2020), "Design of Cold-Formed Ferritic Stainless Steel Unlipped Channels with Offset Web Openings and Unfastened Flanges Subject to Web Bearing Failure Under One-Flange Load Scenarios", *Structures* **27**, 194-211.

Yousefi, A.M., Samali, B. and Hajirasouliha, I. (2020), "Experimental and numerical investigations of cold-formed austenitic stainless steel unlipped channels under bearing loads", *Thin-Wall. Struct.,* **152**, 106768.

Yousefi, A.M., Samali, B. and Yu, Y. (2021), “Shear Behaviour and design of cold-formed ferritic stainless steel channels with circular web openings”, *Structures*, https://doi.org/10.1016/j.istruc.2021.06.093

Yu, Y., Royel, S., Li, Y., Li, J., Yousefi, A.M., Gu, X., Li, S. and Li, H. (2020), “Dynamic modelling and control of shear-mode rotational MR damper for mitigating hazard vibration of building structures”, *Smart Materials and Structures,* **29** (11), 114006.

Yu Y., Rashidi, M., Samali, B., Yousefi, A.M. and Wang, W. (2021), “Multi-Image-Feature-Based Hierarchical Concrete Crack Identification Framework Using Optimized SVM Multi-Classifiers and D–S Fusion Algorithm for Bridge Structures”, *Remote Sensing*, **13**(2), 240. https://doi.org/10.3390/rs13020240.